https://doi.org/ 10.33472/AFJBS.6.9.2024.1213-1227

African Journal of Biological Sciences

Journal homepage: http://www.afjbs.com

Research Paper Open Access

A CNN-based automated diagnosis system for diabetic macular edema

Manisha Bangar[1,*], Prachi Chaudhary[2]

[1] Matu Ram Institute of Engineering and Management, Rohtak, Haryana, India

manishabangar@gmail.com

[2] Deenbandhu Chhotu Ram University of Science and Technology, Murthal, Haryana, India

prachi.ece@dcrustm.org

[*]Corresponding author: manishabangar@gmail.com

Article History

Volume 6,Issue 9, 2024

Received: 26-03-2024

Accepted : 28-04-2024

doi: 10.33472/AFJBS.6.9.2024.1213-1227

Abstract: The application of convolutional neural networks (CNN) for feature extraction and categorization of medical images has advanced to an impressive level. With better architectures and improved parameters, their efficiency is improving day by day. Using optical coherence tomography (OCT) images, this research proposes a CNN-based automated diagnosis system for diabetic macular edema (DME). DME is a significant cause of visual impairment in diabetic patients globally. As a result, it is critical to creating an automated diagnostic system capable of detecting DME symptoms as early as possible. The proposed research compares the performance of three CNNs (a proposed CNN, VGG-16, and DenseNet) for DME classification in two categories: normal and DME. The proposed CNN outperformed VGG-16 & DenseNet with a lower system loss and exceeded significantly in terms of classifier accuracy, precision, f1-score, and receiver operating characteristics (ROC). The proposed CNN obtained classifier accuracy of 90.26%, while VGG-16 & DenseNet obtained 87.41% & 82.66% respectively. The area under ROC for the proposed CNN, VGG-16 & DenseNet is 0.96, 0.96 &0.92 respectively.

Keywords: ***Convolutional neural networks, diabetic macular edema, classification, ROC, optical coherence tomography, ophthalomology***

1. Introduction

Diabetic macular edema (DME) is a vision-threatening condition in which the retinal layers deteriorate over time in diabetic patients with uncontrolled diabetes. According to the studies, the graph of diabetes incidence and prevalence is rising at an alarming rate on a global scale. Every country's age-standardized diabetes prevalence in adults has increased or remained stable since 1980. This increase combined with population growth and aging has nearly quadrupled the number of adults worldwide with

diabetes [1]. Furthermore, the intended age of pathology is decreasing, which is cause for serious concern. The increased glucose level in the blood causes blood vessel impairment, affecting patients' overall health. These complications affect the majority of people with type-1 and type-2 diabetes. Kidney disease, blindness, and amputations are among the most common micro-vascular complications [2]. These impaired blood capillaries in the retinal layers cause fluid leakage outside the capillaries into the retinal space. This leaked content becomes trapped and accumulates between the retinal layers, causing visual health problems. Ophthalmologists refer to this condition as diabetic retinopathy (DR). The deposition of various types of leaked fluid particles causes distinct lesions, such as hemorrhages, exudates, cotton wool spots, and the growth of abnormal blood vessels in the retinal region. Table 1 shows the nature of these pathological features as well as the elements that cause them.

Table 1: Different pathological features appearing on the retina due to diabetes

Sr. No.	Name of pathological feature	Appearance	Texture properties	Inducing factor
1	Hemorrhages	Bright red	Oval/round dot or blot	Broken blood vessel
2	Exudates	Yellow	Spots with sharp edges	Lipid and protein deposit
3	Microaneurysms	Red	Dot type structure	Accumulation of blood near the vessel wall
4	Drusen	Yellow	Dotted tissue growth	Fat deposition reduced the capacity of the retina to cleanse waste from photoreceptors
5	Cotton wool spots	Yellowish/grayish white	Cloud-type lesions edge not clear	Lack of blood flow to smaller blood vessels
6	Macular edema	Retinal layer thickening	Swelling in retinal layers	Presence of pathology near the macular region
7	Abnormal blood vessels	Red	Web-like structure	Growth of abnormal blood vessels

The pathological features mentioned above can appear anywhere on the retina. The location of these features is the most important parameter for patients' visual health. The symptoms of DR include dark or empty spots floating in the vision area, blurred or fluctuating vision, and partial vision loss. It can proceed to complete vision loss if ignored at the initial stage. The severity of vision loss is determined by the location of these features on the retinal layers. Though these lesions can occur anywhere and cause vision loss, the location at or near the macula is particularly critical for vision. The reason for this conclusion is that the macula is the region of the retina with the highest density of rods and cones and thus provides the best and sharpest vision. Any abnormal feature in or near this region harms vision. As a result, diabetic macular edema, despite being a component of DR, is the most substantial of all pathological features. The appearance of any of the pathological features described in Table 1 near the macula is defined as DME. DME conditions are classified into two types, as follows:

- Clinically significant macular edema (CSME) – It is characterized by retinal thickening within 1/3 disc diameter (DD) of the foveal center or the presence of exudates in this area or areas of retinal thickening at least 1 DD in size which is within 1 DD of the center of the macula.

- Non- clinically significant macular edema (non-CSME) - NCSME is a condition of macular edema when the location of exudates and other abnormalities are at a distance from the fovea and the central vision of the subject is not affected.

The treatment and follow-up for DME begin with diabetic patients becoming aware of their visual health. DME can be successfully treated if detected early. According to surveys and studies, in some countries, patients are unaware of the diabetes-related complications in their bodies. On the other side, in other countries, despite high levels of awareness about diabetic eye diseases, a significant proportion of diabetic patients failed to report an annual eye examination [3]. As a result, it is consistently reported to ophthalmologists when the condition has progressed to an irreversible state. As a result, keeping a record and following up on the visual health of diabetic patients has become difficult for ophthalmologists. Furthermore, with the rising prevalence of diabetes, it is already a burden on doctors to treat and restore patients' visual health. With the rising worldwide prevalence of diabetes and DR, public healthcare systems across both developed and developing nations will face rising costs for implementing and maintaining diabetes and DR monitoring program. To lessen the impact of DR-related vision loss, all stakeholders must keep seeking innovative ways to manage and prevent diabetes, as well as optimize cost-effective examinations in the community [4].

The key to better treating and restoring diabetic patients' visual health is automated DME diagnosis. This study explains and proposes a convolutional neural network-based (CNN-based) automated diagnostic system for DME. An automated diagnosis system for DME detection can not only reduce the burden on ophthalmologists, but it can also provide a precise analysis of pathology using efficient image processing tools. Figure 1 depicts the basic task flow for an automated DME diagnostic system.

Figure 1: Steps for automated diagnosis system for DME

Contributions:

- This study proposes a CNN-based automated diagnosis and classification system capable of classifying any given optical coherence tomography (OCT) image as normal or abnormal.
- The study is carried out with secondary data for classifier design and implementation. The acquired images are pre-processed to ensure that the dataset is uniform in terms of size, resolution, and noise reduction.
- The pre-processed images are subjected to k-means clustering with structural similarity (SSIM), which separates the OCT images into retinal layers and background pixels.
- The segmented images are then divided into training and testing data, allowing CNN to be trained to classify images into two categories: normal and abnormal.

- The performance of the trained CNN is then tested and validated. The novelty of this study is that it consists of a performance comparison of the proposed CNN with two pre-trained CNN concluding the best of three.

The following is how this paper is organized: The first section is the introduction, which contains background information about the concept. Section 2 is a review of related literature. The proposed methodology is presented in Section 3. Section 4 contains the result and experimental details. Section 5 is devoted to discussion and conclusions.

1. Related literature

Automated diagnosis systems for early detection of DME have been an area of interest for people working on artificial intelligence for the last decade. Research has been carried out, and prototypes have been designed for a universal DME screening system. Manisha et al. concluded in a comparative analysis of automated detection systems for DME that the classifier accuracy depends on many factors like the size of the dataset, image quality, grading levels, noise factor, etc. [5]. Machine learning and other soft computing techniques have demonstrated the ability to classify medical images on par with human experts. It has been found in several studies so far, though the systems are prototypes only and could not be used commercially due to some inherent inconsistencies.

The evolution of CNN has marked an endless development in data analysis and processing. Classification and pattern recognition are the most desirable application areas for CNNs. Deep CNN is more accurate in its learning and classification of given data. Exploiting the same approach, Pratt et al. suggested the use of a deep neural network for DR classification with a large dataset [6]. For a 5-grade classification, the suggested deep learning algorithm achieved a classifier accuracy of 75%. Deep CNN Inception-3 is proposed by Gulshan et al. as a classifier for two different datasets, and different classifier accuracy was found with both datasets [7]. Grassmann et al. proposed the incorporation of a random forest classifier with a deep CNN for 13-grade classification [8]. Deep CNN is also favored by Perdomo et al. for the diagnosis of DME; the algorithm was based on five features and achieved an accuracy of 93.75%. [9].

The use of CNN comes with training and testing phase. It is apparent that to achieve high classifier accuracy, the dataset used should be large and provide sufficient diversity in features. The appropriate datasets also necessitate a significant amount of time in both the training and testing phases. To rectify the situation, transfer learning is employed, where a pre-trained CNN is fine-tuned for the desired dataset; in this way, CNN can perform well even with a smaller dataset. Transfer learning is proposed by Kermany et al. to make a CNN-based classifier fast and comparably accurate. When tested on a small and larger dataset, the pre-trained CNN achieved an accuracy of up to 96.6% [10]. Karri et al. proposed a similar approach of transfer learning with some modifications and achieved classifier accuracy of up to 99% [11]. It suggested back propagation for the rectification of the filters. The proposed system performed better in terms of accuracy, but the sensitivity and specificity were significantly degraded. Kamble et al. concluded that they achieved 100% accuracy on a small dataset by fine-tuning a pre-trained CNN to classify normal and abnormal eyes [12].

Giancardo et al. proposed using probabilistic, geometric, and tree-based classification as well as wavelet-based feature extraction to achieve an area under the curve of 0.88–0.94 [13]. A supervised learning-based neural network was suggested by Acharya et al. [14] and Deepak et al. [15]. Srinivasan et al. implemented an support vector machine (SVM) classifier to classify normal, DME, and age-related macular degeneration (AMD) with histogram-based feature extraction and obtained 86.7% accuracy to detect a normal eye and 100% accuracy to detect DME and AMD [16]. The SVM classifier with CNN-based feature extraction proposed by Genevieve et al. attained a classification accuracy of 96% [17].

A novel DME classifier was proposed by Manisha et al. that combined a support vector machine classifier with a discrete wavelet transform as a feature extraction technique to achieve an overall accuracy of 96.46% [18]. Wang et al. proposed a deep learning-based classifier for age-related macular edema and DME, concluding that CliqueNet outperformed others with an accuracy of 98% and an area under the curve of 0.99 [19].

Alsaih et al. proposed a machine-learning DME classifier for spectral domain OCT with combined feature extraction (principle component analysis features and linear binary pattern features) and a support vector machine classifier, achieving 87.5% sensitivity and specificity [20]. Barua et al. created a multilevel deep feature extraction framework for OCT images with an optimized classifier that achieved classifier accuracy of 97.40% and 100% for two different databases [21]. Sunija et al. proposed a deep CNN for grading choroidal neovascularization, DME, and drusen in OCT images. The proposed CNN achieved 99.69% accuracy [22].

2. Proposed methodology

Figure 1 depicts the basic flow of work in the automated detection of DME, which uses various techniques for image processing for image classification. The following are the procedures:

3.1 Data collection

This study relied on publicly available OCT data. The data was obtained from the Kaggle depository, an online open-source directory. A total of 3000 images were accessed from kaggle.com, with 124 images being discarded due to poor contrast and unacceptable levels of noise. For the study, 2876 OCT images were saved. There are 958 images in this dataset that belong to the DME case and 1918 images that belong to the normal case. The dataset was divided into two parts after pre-processing and segmentation: training and testing data. The CNN was trained using 2455 images, and 421 images were used for testing and validation. The dataset configuration is depicted in Figure 2.

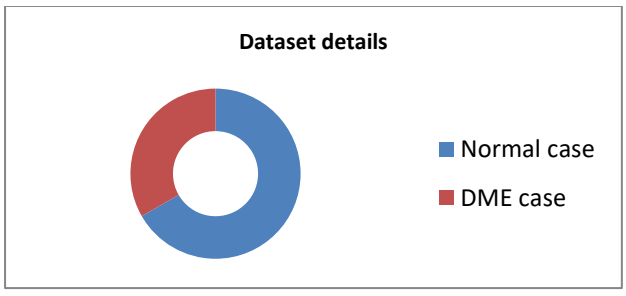

Figure 2: Dataset configuration

2.1 Pre-processing

The secondary data obtained from public sources are raw and poorly organized. As a result, the dataset must be prepared consistently in terms of image size and contrast level. Images are pre-processed before segmentation to achieve dataset uniformity. To create a uniform dataset, image resizing, and cropping are used. Image size is very important in CNN training and testing. Larger image sizes necessitate more memory and take more time to train, whereas smaller image sizes result in poor feature extraction. As a result, it is crucial to choose an optimum image size that retains the necessary features without demanding too much time during CNN training and testing. The images have been resized to an optimum size of 128x128 for further processing. Figure 3 shows a pre-processed OCT scan with a normal case.

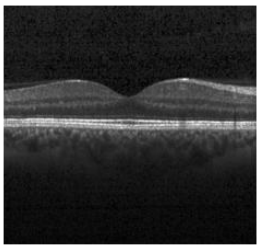

Figure 3: Normal eye OCT scan after image cropping and resizing

2.2 Image segmentation

The most important step in automated detection is image segmentation. During this stage of image processing, the image pixels are partitioned into featured pixels and background pixels. As a result, the image indicates the forefront information with regard to the background data. It aids in more accurate and precise feature extraction in the following processing step. In this study, the K-means clustering with structural similarity (SSIM) feature is used for image segmentation because it efficiently segments OCT images. Clustering algorithms divide unorganized data into k categories based on similar contrast or energy levels, with the user defining the value of k. Initially, the segmentation is performed with the value k=4. As a result, the images are divided into four clusters. Figure 4 shows a segmented image where k = 4. The algorithm arranges the pixels into four clusters, as shown in the image.

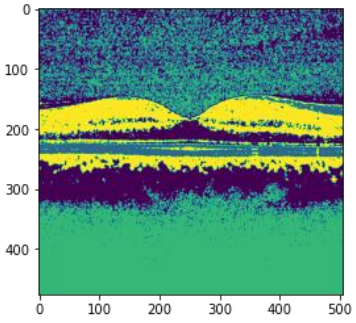

Figure 4: Segmented image using k-means clustering with k=4

Following image segmentation, the SSIM feature is used to select the most relevant cluster type suitable for feature extraction. To determine the best cluster composition for feature extraction, the SSIM feature compares the clusters to a previously provided reference image. Figure 5 depicts the distinct cluster structure with respect to the background that is going to be compared by the SSIM feature.

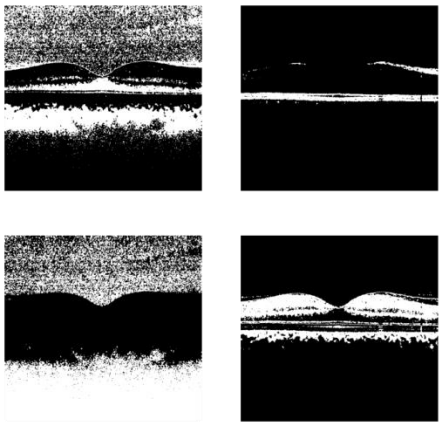

Figure 5: Individual cluster and a background view of the segmented image

2.3 Feature extraction and classification

This study proposes CNN-based feature extraction and classification. Transfer learning is used to fine-tune two pre-trained CNNs, VGG-16 and DenseNet, on an OCT dataset, and a new CNN is proposed for the automated detection of DME using OCT images. The followings are the architectural details and CNN tuning parameters:

Proposed CNN

The proposed CNN is a 20-layer architecture consisting of 5 convolutional layers, pooling layers, and dropout layers. After the fifth dropout layer, there is one flatten layer followed by three dense layers, also known as fully connected layers. Figure 6 depicts the systematic arrangement of layers as well as their respective feature maps. The activation function for convolution layers is ReLU (the Recti-Linear function), and the last layer is SoftMax. ADAMAX is the optimizer used, and the learning rate is set to 0.001. The comparison of CNNs in terms of parameters is summarized in Table 2.

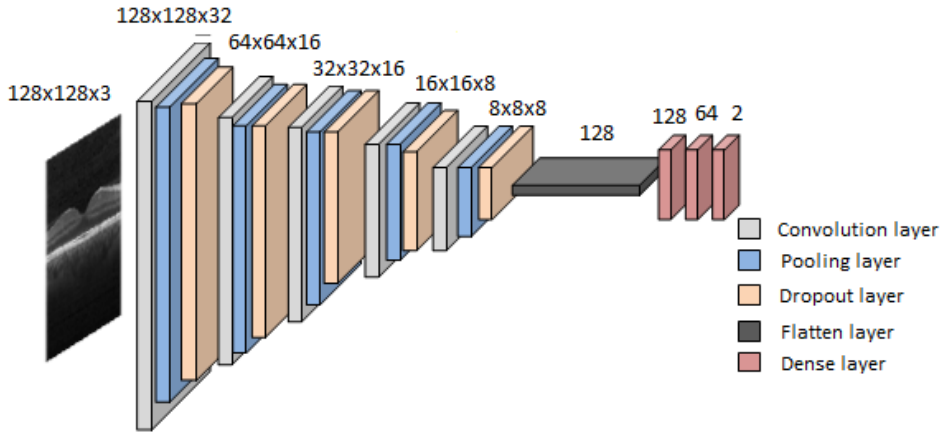

Figure 6: Architecture of proposed CNN

VGG-16

VGG-16 is a publicly available pre-trained CNN trained on general (non-medical) datasets. Transfer learning is used to fine-tune over the intended data for this study. It has a total of 21 layers, which include 13 convolutional layers, 5 pooling layers, 1 dense layer, 1 input layer, and 1 flattening layer. Figure 7 depicts the layer arrangement and feature map for VGG-16. Table 2 lists the tuning parameters for all three CNNs.

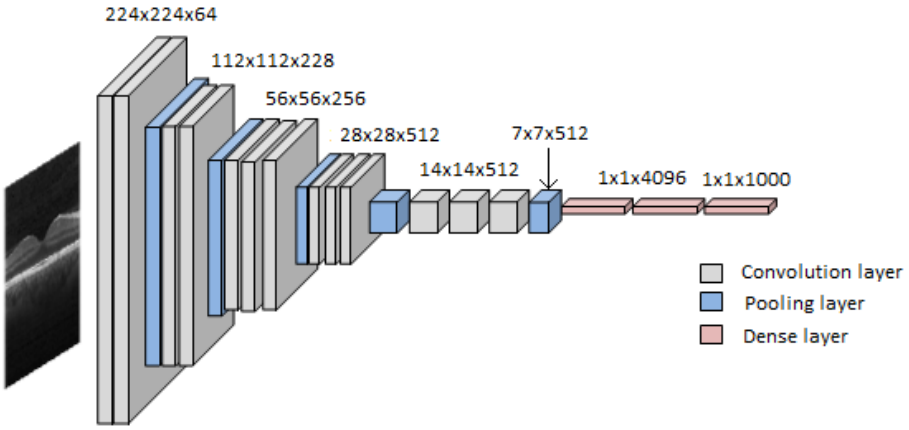

Figure 7: Architecture of VGG-16

DenseNet

DenseNet is a 121-layer deep CNN that has been pre-trained on general data. It is also fine-tuned for OCT target data using transfer learning. It is made up of four dense blocks, three transition layers, one input layer, and one classification layer. The dense blocks are a repetitive layered structure of a sequenced batch normalization layer, ReLU, convolution layer, and dropout layer. Table 2 lists the other architectural details and fine-tuning parameters.

Table 2: Architectural details of used CNN

Parameters	**Proposed CNN**	**VGG-16**	**DenseNet**
Total no. of layers	20	21	121
Convolutional layers	5	13	1
Pooling layers	5	5	1
Other layers	1 input, 5 dropout layers (dropout-20%), 1 flatten layer, 3 dense layers	1 input, 1 flatten layer, 1 dense layer	1 input, 4 Dense blocks, 3 transition layers, 1 classification layer
No. of trainable parameters	29,202/29,202	50,178/14,714,688	2,050/7,039,524

Activation function	Relu, softmax on last dense layer	softmax	softmax
Learning rate	0.001	0.001	0.001
Optimizer	Adamax	Adamax	Adamax
Input	128x128x32	224x224x3	224x224x3
loss	Categorical cross-entropy	Categorical cross-entropy	Categorical cross-entropy
Training testing batch size	16	16	16
epochs	50/50	9/20	8/20
time	6 sec	3 sec	2 sec

2.4 Performance evaluation parameters

Several parameters, including classifier accuracy, precision, recall, and area under the ROC (receiver operating characteristic) curve, are used to assess the performance of the proposed method. The following are the parameters:

Accuracy

The accuracy of a classification model is a metric of its performance. It is commonly expressed as a percentage. It is the number of predictions in which the predicted value is equal to the true value.

$$Accuracy = \frac{True\ Positive + True\ Negative}{True\ Positive + True\ Negative + False\ Positive + False\ Negative}$$

Precision

It is calculated as the ratio of the number of correctly classified positive samples to the total number of positive samples (either correctly or incorrectly classified). The precision of the model measures its accuracy in classifying a sample as positive.

$$Precision = \frac{True\ Positive}{True\ Positive + False\ Positive}$$

Recall

It is calculated as the ratio of positive samples that were correctly classified as positive to the total number of positive samples. The recall of the model measures its ability to detect positive samples.

$$Recall = \frac{True\ Positive}{True\ Positive + False\ Negative}$$

Loss function

It is also referred to as the cost function. It considers the probability or uncertainty of a prediction based on how far the prediction deviates from its true value. Log loss, cross-entropy loss, mean square error, and likelihood loss are the most common loss functions.

Here, Mean squared error is used as a loss function. Mathematically,

$$L = (T - P)^2$$

Where, L = Loss function
T = True value
P = Predicted value

Receiver Operating Characteristics (ROC)

ROC is a graph that depicts a classification model's performance across all classification thresholds. The true positive rate and the false positive rate are plotted on this curve. The area under the ROC curve (AUC) is a critical parameter. It has a value between 0 and 1. A model with 100% incorrect predictions has an AUC of 0.0; one with 100% correct predictions has an AUC of 1.0.

3. Results

Following the implementation of the proposed algorithms, the performances of the proposed CNN, VGG-16, and DenseNet are compared in terms of ROC, classifier accuracy, precision, recall, loss function, and f1-score. Figures 8, 9, and 10 show the ROC curves for the proposed CNN, VGG-16, and DenseNet. The proposed CNN and VGG-16 both achieved 96% area under the curve for classes 0 (normal eye) and 1 (DME) and outperformed DenseNet, which obtained 92% for the same. The analysis of ROC curves shows that the proposed CNN fared better in terms of area under the ROC.

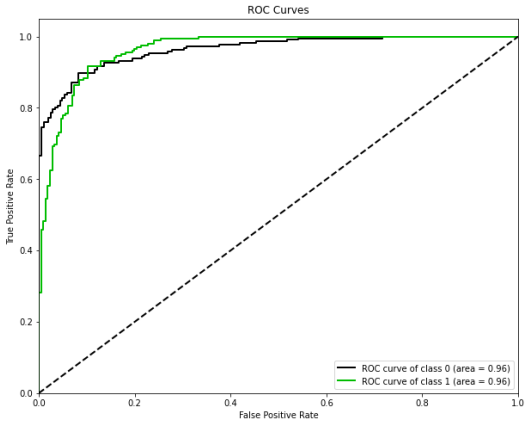

Figure 8: ROC for proposed CNN

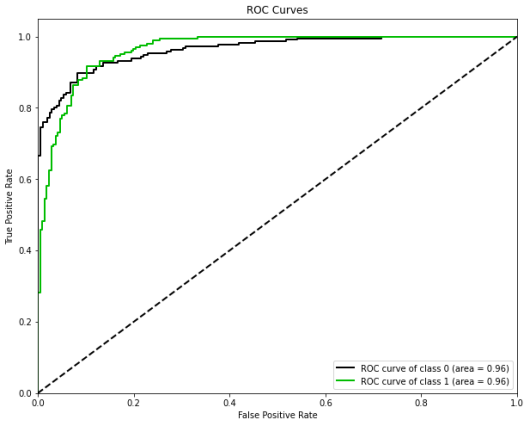

Figure 9: ROC for VGG-16

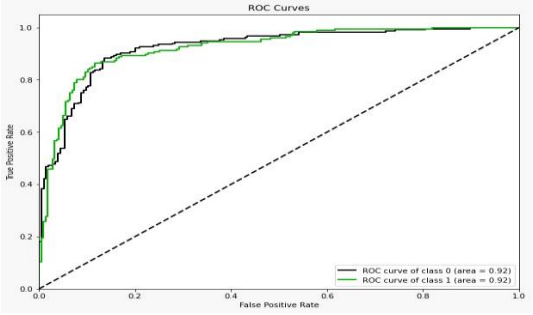

Figure 10: ROC for DenseNet

The confusion matrix obtained to evaluate classifier performance for predicted class correctness is shown in the figures below. Figure 11 depicts the proposed CNN's confusion matrix, while figures 12 and 13 depict the same for VGG-16 and DenseNet, respectively. Tables 3, 4, and 5 show the other evaluation parameters derived from the confusion matrix, such as precision, recall, and f1-score. Table 6 compares the performance of three CNNs and concludes that the proposed CNN performed the best of the three in terms of the majority of parameters. Table 7 compares the performance of the proposed work to that of other studies.

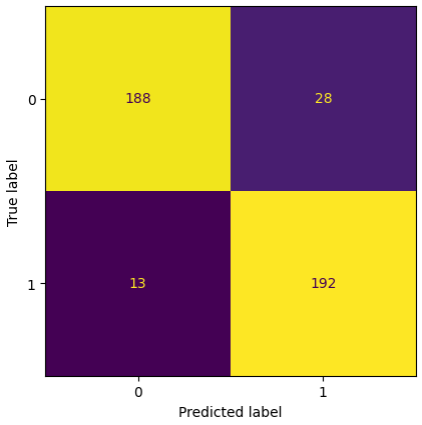

Figure 11: Confusion matrix for proposed CNN

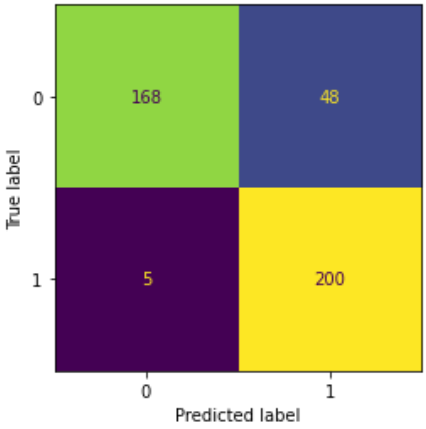

Figure 12: Confusion matrix for VGG-16

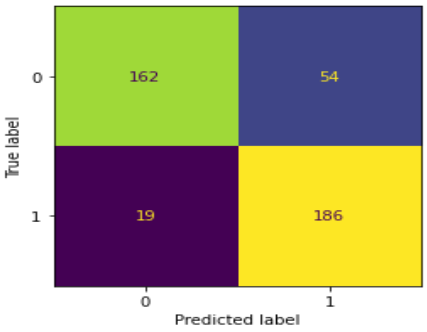

Figure 13: Confusion matrix for DenseNet

Table 3: Performance of proposed CNN

Performance: Proposed CNN				
	Precision	Recall	F1-score	support
Normal eye class 0	0.86	0.96	0.90	201
DME eye class 1	0.89	0.87	0.91	220
Accuracy			0.90	421
Macro avg	0.87	0.94	0.90	421
Weighted avg	0.88	0.93	0.90	421

Table 4: Performance of VGG-16

Performance: VGG-16				
	Precision	Recall	F1-score	support
Normal eye class 0	0.78	0.97	0.86	173
DME eye class 1	0.98	0.81	0.88	248
Accuracy			0.87	421
Macro avg	0.88	0.89	0.87	421
Weighted avg	0.89	0.87	0.88	421

Table 5: Performance of DenseNet

Performance: DenseNet				
	Precision	Recall	F1-score	support
Normal eye class 0	0.75	0.90	0.82	181
DME eye class 1	0.91	0.78	0.84	240
Accuracy			0.83	421
Macro avg	0.83	0.84	0.83	421
Weighted avg	0.84	0.83	0.83	421

Table 6: Performance comparison of CNNs

Performance Analysis of all CNNs						
CNN	Precision	Recall	f-score	Accuracy (%)	ROC	LOSS
Proposed CNN	**0.87**	**0.94**	**0.90**	**90.26**	**0.96**	**0.2964**
VGG-16	0.89	0.87	0.88	87.41	0.96	0.3621
DenseNet	0.84	0.83	0.83	82.66	0.92	0.3844

Table 7: Performance comparison of proposed work

Sr. No.	**Related work**	**Technique**	**Classifier accuracy (%)**
1	Pratt et al. [6]	Deep CNN	75
2	Perdomo et al. [9]	CNN without dropout	81.25
3	Srinivasan et al. [16]	HOG + SVM	86.7
4	Proposed work	Proposed CNN	**90.26**

4. Conclusion

We present an efficient transfer learning-based approach for automated detection and classification of DME using OCT images in this study. The classification is divided into two categories: normal and DME. The purpose of this research is to reduce the burden on ophthalmologists and to propose a screening system for detecting DME symptoms using OCT scans. This work is unique in that it uses two steps of image segmentation to prepare training data for CNNs, resulting in better feature extraction and higher classifier accuracy. The clustering algorithm is a widely used segmentation method, and this study

employs it along with the SSIM feature. The use of a similarity index in image segmentation resulted in more precise and accurate image segmentation. CNN is used for classification. A novel 20-layer CNN is proposed for OCT scan classification, along with two pre-trained CNNs (VGG-16 and DenseNet) that are fine-tuned using transfer learning for our target dataset.

For the best classifier, the performance of three CNNs is compared. The proposed CNN outperformed VGG-16 and DenseNet despite having a simpler architecture, providing a classifier accuracy of 90.26% while VGG-16 achieved an accuracy of 87.41% and DenseNet achieved an accuracy of 82.66%. Precision, recall, f1-score, and area under ROC are also analyzed for all three CNNs, the proposed CNN, VGG-16 and DenseNet. The values of precision for the proposed CNN, VGG-16, and DenseNet are 0.87, 0.89, and 0.84, respectively. The recall factor was recorded as 0.94 for the proposed CNN, 0.87 for VGG-16 and 0.83 for DenseNet. Though the precision value obtained by VGG-16 exceeds the other two CNNs, the overall performance analysis of the three CNNs shows the best performance by the proposed CNN. The proposed CNN possesses a 0.022 lower loss function than VGG-16 and a 0.088 lower loss function as compared to DenseNet. The proposed CNN outperformed in terms of the majority of parameters, with a classifier accuracy of 90.26%, a precision of 0.87, a recall of 0.94, an f1-score of 0.90, an area under the ROC of 0.96, and a loss function of 0.2964. As a result, it is concluded that the proposed CNN achieved the best performance. Though the goal of this research is to provide an efficient automated diagnostic system for DME at the screening level, it can be further improved for a larger dataset and more than two classes of classification.

Declarations

Competing interests
The authors have no competing interests to declare that are relevant to the content of this article.

Authors' contributions
Manisha Bangar conceived the idea, design and drafting of the study. Prachi Chaudhary collected and analyzed the data. All authors have reviewed the manuscript.

Funding
No funding was received for conducting this study.

Availability of data and materials
The data analyzed during this study can be found at www.kaggle.com at the given link: (https://www.kaggle.com/paultimothymooney/kermany2018).

References

[1] Zhou BLY, Hajifathalian K, Bentham J, Di Cesare M, Danaei G, Bixby H. Worldwide trends in diabetes since 1980: a pooled analysis of 751 population-based studies with 4.4 million participants. Lancet (London England). 2016; 387(10027): 1513-30. https://doi.org/10.1016/s0140-6736(16)00618-8.

[2] Forbes JM, Cooper ME. Mechanisms of diabetic complications. Physiol Rev. 2013;93(1):137–88. https://doi.org/10.1152/physrev.00045.2011.

[3] Konstantinidis et al. BMC Endocrine Disorders (2017) vol. 17, DOI 10.1186/s12902-017-0206-2

[4] Ting DS, Cheung GC, Wong TY. Diabetic retinopathy: global prevalence, major risk factors, screening practices, and public health challenges: a review. Clinical & experimental ophthalmology. 2016;44(4):260–77. https://doi.org/10.1111/ceo.12696.

[5] Manisha, Prachi Chaudhary: Automated Diagnosis of DME: A Comparative Analysis. International Journal of Advanced Research in Engineering and Technology. Volume 11. Issue 12. pp. 446-456 (2020).

[6] Harry Pratt et al.: Convolutional Neural Networks for Diabetic Retinopathy. International Conference on Medical Imaging Understanding and Analysis 2016, Procedia Computer Science 90 (2016) 200-205, (2016) Elsevier

[7] Varun Gulshan et al.: Development and Validation of Deep Learning Algorithm for Detection of Diabetic Retinopathy in Retinal Fundus Photographs. Original Investigation, (2016) American Medical Association

[8] Felix Grassmann et al.: A Deep Learning Algorithm for prediction of age-related eye disease study severity scale for age-related macular degeneration from color fundus photography. American Academy of Ophthalmology, (2018)

[9] Perdomo et al.: OCT-NET: A Convolutional Network for Automatic Classification of Normal and Diabetic Macular Edema using SD-OCT Volumes. IEEE 15th International Symposium on Biomedical Imaging (ISBI 2018).

[10] Daniel S. Kermany et al.: Identifying Medical Diagnosis and Treatable Diseases by Image-based Deep Learning. Cell 172 (2018) Elsevier, 1122-1131.

[11] S.P. K. Karri et al.: Transfer Learning based classification of Optical Coherence Tomography images with Diabetic Macular Edema and dry Age-Related macular degeneration. Biomedical Optics Express 579 Vol. 8, No. 2, (2017).

[12] Kamble et al.: Automated Diabetic Macular Edema (DME) Analysis using Fine Tuning with Inception-Resnet-v2 on OCT Images. IEEE-EMBS Conference on Biomedical Engineering and Sciences (IECBE 2018)

[13] Giancardo et al.: Exudate-based diabetic macular edema detection in fundus images using publically available datasets. Medical Image Analysis 16 (2012) 216-226.

[14] U. Rajendra Acharya et al.: Automated Diabetic Macular Edema grading system using DWT, DCT features and Maculopathy Index, Computers in Biology and Medicine. (2017) May 1;84:59-68;. doi:10.1016/j.compbiomed.2017.03.016

[15] Deepak et al.: Automatic Assessment of Macular Edema from Color Retinal Images. IEEE transactions on medical imaging. VOL. 31, No. 3, (2012).

[16] Pratul P. Srinivasan et al.: Fully Automated Detection of Diabetic Macular Edema and dry age-related macular degeneration from optical coherence tomography images. Biomedical Optics Express 3568 Vol. 5 N0.10 (2014) OSA

[17] Genevieve et al.: Transfer Learning for Diabetic Macular Edema (DME) Detection on Optical Coherence Tomography (OCT) Images. Proceedings of the 2017 IEEE International Conference on Signal and Image Processing Applications (2017), Malaysia

[18] Manisha Bangar, Prachi Chaudhary,; A novel approach for the classification of diabetic maculopathy using discrete wavelet transform and a support vector machine. AIMS Electronics and Electrical Engineering. Volume 7. Issue 1. pp 1-13. (2022).

[19] Depeng Wang, Liejun Wang,; On OCT image classification via deep learning. IEEE photonics journal. Volume 11, Issue 5. (2019).

[20] Khaled Alsaih et al.; Machine learning techniques for diabetic macular edema (DME) classification on SD-OCT images. Biomedical Journal Online. 16:68. pp 1-12. (2017).

[21] Prabal Datta Barua et al.; Multilevel deep feature generation framework for automated detection of retinal abnormalities using OCT images. Entropy. 23, 1651. pp 1-18. (2021).

[22] Sunija A P et al.; OctNet: A lightweight CNN for retinal disease classification from optical coherence tomography images. Computers methods and programs in biomedicine. (2020).